ADVANCED MATERIALS
www.advmat.de

Thermal Management by Engineering the Alignment of Nanocellulose

Ivan I. Smalyukh

One of the grand current research challenges is to improve the energy efficiency of residential and commercial buildings, which cumulatively consume more than 40% of the energy generated globally. In addition to improving the comfort of the inhabitants and mitigating the growing energy consumption problem, new building materials and technologies could provide a safe strategy for geoengineering to mitigate global climate change. Herein, recent progress in developing such advanced materials from nanocellulose, which is often derived from wood or even dirty feedstocks like waste, is reviewed. By using chemical and bacteria-enabled processing, nanocellulose can be used to fabricate broadband photonic reflectors, thermally super-insulating aerogels, solar gain regulators, and low-emissivity coatings, with potential applications in windows, roofs, walls, and other components of buildings envelopes. These material developments draw inspiration from advanced energy management found in nature, such as the nanoporous photonic structures that evolved in cuticles of beetles. Fabrication of such materials takes advantage of mesoscale liquid crystalline self-assembly, which allows for pre-designed control of cellulose nanoparticle orientations at the mesoscale. With the potential fully realized, such materials could one day transform the current energy-lossy buildings into energy plants on Earth and possibly even enable extraterrestrial habitats.

1. Introduction

Nanoporous periodic structures are abundant in nature and common to many forms of life, ranging from beetles to crabs, fish and birds,[1–6] and are even found in fossils of dinosaurs.[7–15] Well-preserved fossils, often over 500 million years old, reveal the important role of such structures in evolution.[7–15] The orderly mesoscale features evolved to enable selective and broadband reflections of solar radiation and thermal energy management under often harsh ambient conditions, in addition to other survival-related needs.[7–15] Historically, they attracted a great deal of interest among researchers. For example, such structures were studied by Hooke and Newton several centuries ago.[16,17] Michelson, years after his famous measurement of the speed of light, studied metallic colors and vivid reflections in insects and birds.[18] The modern understanding of the origins of the visible and infrared photonic reflections in nature[1] benefited from direct nanoscale imaging and the recent development in theoretical modeling and experimental realization of photonic crystals and metamaterials.[19] Although the structures reflecting light in the visible spectral range attracted the strongest research interest, it was also noted that many photonic structures in nature reflect in the near infrared range (responsible for over 50% of energy due to solar radiation that tends transforming to heat), typically to enable thermal management for birds, beetles and so on.[2,4–6] Certain ants, like *Cataglyphis bombycina*, survive under extreme temperature conditions not only using broadband visible and near-infrared reflection (responsible for their silvery appearance), but also by dissipating heat via radiative cooling.[20] While various photonic and metamaterial designs have been developed recently to robustly control selective or broadband reflectivity and for radiative cooling, nature keeps surprising us by revealing similar thermal management solutions.[20–22] Such biological solutions for thermoregulatory problems, many of which remain to be discovered and understood, are important for inspiring the development of biomimetic and bioderived building materials that will be the focus of this brief review.

The technological needs of thermal management in modern buildings are largely reminiscent to those faced by diverse forms of life on Earth over hundreds of millions of years. The sun remained relatively the same, most important energy resource on Earth over this period of time, as did the ambient temperatures on Earth's surface (with some geographic and temporal variations).[20,22] Consequently, nature's thermal management solutions can be adopted in developing more efficient building materials. Various photonic reflectors and thermal

Prof. I. I. Smalyukh
Department of Physics
Department of Electrical
Computer and Energy Engineering
Materials Science and Engineering Program
and Soft Materials Research Center
University of Colorado
Boulder, CO 80309, USA
E-mail: ivan.smalyukh@colorado.edu
Prof. I. I. Smalyukh
Renewable and Sustainable Energy Institute
National Renewable Energy Laboratory and University of Colorado
Boulder, CO 80309, USA
The ORCID identification number(s) for the author(s) of this article can be found under https://doi.org/10.1002/adma.202001228.

DOI: 10.1002/adma.202001228

barriers found in nature can be mimicked to produce energy-efficient building materials for applications in windows, walls, roofs and other parts of building envelopes. Such materials can be made from the most abundant biopolymer, cellulose, when derived from wood and even from dirty initial feedstocks like waste.[23–25] These bioinspired material designs can not only allow for more efficient energy uses, but also may enable solar heat harvesting, effectively transforming the current energy-consuming buildings into power plants in the future. Moreover, the energy management within buildings can be combined with safe geoengineering[26] to mitigate the global climate change and local heat waves (especially in urban areas) by reflecting the excess solar radiation back into the space. While this research news mainly focuses on tunable solar reflectors and passive thermal barriers,[23–25,27–31] we note that the capabilities of radiative cooling can be potentially also added to these designs, including the ones based on wood-derived naturally aligned cellulose.[32,33] While being developed to solve energy management problems here on Earth, various thermal management solutions are also needed for the exploration of space, like in extraterrestrial habitats.[34]

Being responsible for over 40% of energy overall, buildings in the USA account for the consumption of 54% of natural gas and more than 70% of electricity.[35,36] Nearly 80% of the building energy is currently derived from the fossil fuels, contributing over 30% of the greenhouse gas emissions.[35,36] US buildings alone are responsible for 40 quadrillion Btu (quads) of energy, much more than the electric energy generated by all US nuclear power plants. At the same time, over one million of new buildings are added each year just in the USA. Since the average buildings stand for over 70 years, with many historic buildings in need of preservation and older buildings being responsible for a large fraction of the wasted energy in the building sector,[35,36] it is also important to develop materials and technologies suitable for effective retrofitting of old buildings without altering their appearance. This review discusses cellulose-based materials intended for uses in both new buildings and in retrofits, with the focus on thermal management by engineering the mesoscale ordering of nanocellulose through utilizing liquid crystal (LC) self-assembly like that found in nature[37–39] and in man-made cellulose nanomaterials.[40–46]

2. Next Generation of Buildings and Mesostructured Materials from Nanocellulose

A building envelope physically separates its conditioned interior from the environment in the exterior, including air flows, water, heat, light and sound transfer (**Figure 1**).[35] To achieve this while minimizing the energy consumption, one needs to achieve thermos-like capabilities of maintaining the desired building's environment without supplying energy regardless of the conditions outside (Figure 1a). Much like in the thermos, it is commonly key to minimize the interior-exterior exchange of energy through thermal conduction, convection and emission.[35] This requirement defines the desired building material characteristics related to thermal conduction and transmission or reflection of electromagnetic radiation in different spectral ranges.[35,36] Since all objects at finite temperatures emit thermal radiation, the conditioning of building's interior and function of envelope components like windows require achieving pre-designed reflection or transmission in different spectral ranges (Figure 1b).[35,36] The sun is the most important energy source at the Earth's surface corresponding to blackbody radiation at about 6000 K, with the atmospheric absorption accounted for (Figure 1b). The other most relevant to building energy consumption is the thermal radiation of the conditioned building's interior at room temperature (inset of Figure 1b).[35,36] All heat sources and sinks can exchange energy through thermal radiation. While a thermos minimizes such an exchange of energy via broadband reflection of thermal radiation from different sources using metal or silvered surfaces, doing this in a building is significantly more difficult because different components of its envelope (like windows and skylights, Figure 1a) have functions often partly incompatible with this need. Likewise, vacuum within double-walled envelope of thermos minimizes energy loss through thermal conduction but taking advantage of vacuum insulation within the building's envelope is not easy. Maintaining a desired conditioned environment within poorly insulated buildings comes at high costs. Figure 1c shows an infrared image that reveals how energy simply leaks through building's envelope on a winter day, especially through the single-pane windows. Constructed over half century ago, its plain-glass single-pane windows and walls have measured R-values of 0.92 and 5.5, respectively. While modern buildings have significantly better envelopes, with *R*-values within 2–5 for windows and 12–21 for walls, a considerable fraction of building energy still escapes.[35,36] To reduce these energy losses, one needs to develop highly insulating, low-thermal-conductivity materials capable of controlling transmission and radiation of electromagnetic waves in the relevant spectral range (Figure 1b). For example, although multi-pane windows with high-performance low-emissivity coatings can achieve R-5 (in some cases even R-10), they are expensive, not fully transparent, hard to install, often structurally incompatible (especially with old buildings, like the one in Figure 1c), have limited deployment and only partially solve the energy loss problem. Using vacuum in some of the window designs to achieve low thermal conductivity and high *R*-values causes problems with seal integrity and long-term durability.[35] Therefore, while modern building materials are more energy-efficient than those from the past,[35,36] a significant room for their improvement and deployment still remains, along with challenges of boosting efficiency of existing buildings through retrofitting.

Nature teaches us a lesson in designing materials that could not only meet high energy efficiency criteria, but also combine function with the aesthetic appeal.[1,47–52] Figure 1d shows two beetles (*Chrysina resplendens* gold scarab beetle and *Chrysina chrysargyrea* silver scarab beetle) with noble-metal-like reflections due to mesoscale structures in cuticles.[3,4,51] These and other beetles are used in jewelry because of the beautiful gold- and silver-like reflections achieved without using noble metals, but they also reflect infrared light,[4,47] as needed for thermal management. Certain types of beetles exhibit photonic structures capable of reflecting only circularly polarized light of one handedness whereas others reflect both left- and right-handed circularly polarized light, with near-100% ambient light

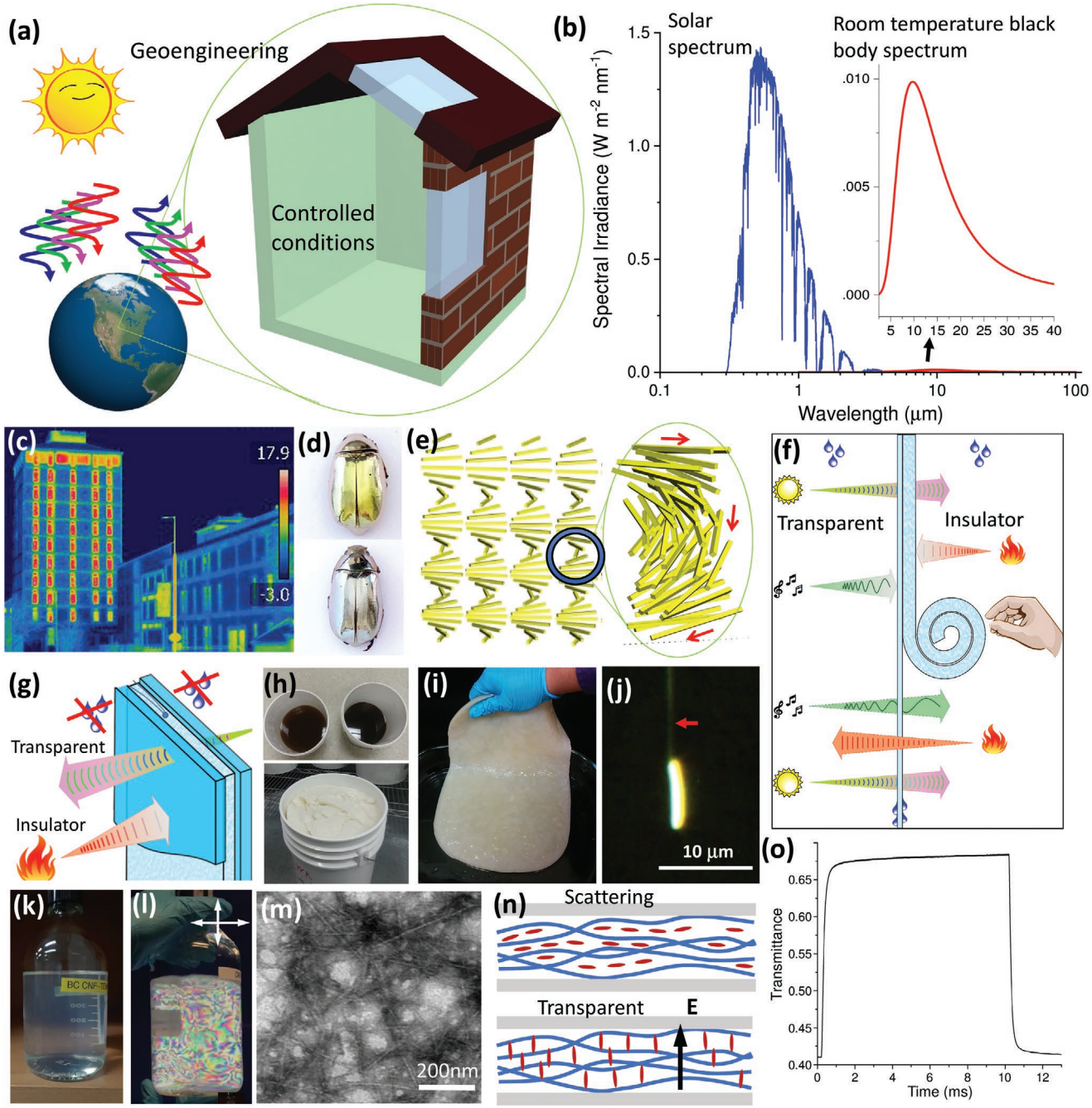

Figure 1. Bioinspired thermal management in buildings using nanocellulose. a) Buildings materials need maintaining conditioned environment in their interior at minimal energy consumption while contributing to geoengineering strategies, e.g., by reflecting excess solar energy. b) Solar spectrum at Earth's surface and (inset) thermal spectrum of room-temperature blackbody radiation. c) Infrared photograph of Gamow Tower in Boulder, Colorado, with the color-coded temperature (in degrees Celsius) scale shown in the right-side inset. d) Photographs of *Chrysina resplendens* gold scarab beetle (top) and *Chrysina chrysargyrea* silver scarab beetle (bottom). e) Schematic of a cholesteric structure formed by cellulose nanocrystals and mimicking that in cuticles of beetles. f) Schematic of thermally insulating low-emissivity film used to retrofit single-pane windows to provide thermal insulation, condensation resistance and soundproofing without compromising visible-range optical transparency. g) Double-pane insulating glass unit with the air gap substituted by a transparent aerogel to provide the same benefits as the retrofitting film in (f). h) Buckets with waste of beer production (top) and never-dried wood pulp (bottom) as initial material sources of nanocellulose. i) Bacterial cellulose pellicle produced from waste shown in (h). j) Bacterium *Acetobacter hasenii* producing cellulose nanofibers that hydrogen-bond to result in a microfiber (marked by an arrow) seen due to light scattering from it. k,l) A lyotropic colloidal LC formed by cellulose nanofibers as observed without (k) and between (l) crossed polarizers (white double arrows). The nanocellulose concentration is ≈1 wt%, with the oxidation utilizing 2,2,6,6-tetramethylpiperidine-1-oxyl radical under mild pH aqueous conditions, as described in details in ref. [24]. m) A TEM image of negatively stained individualized cellulose nanofibers like the ones forming the lyotropic LC shown in (k) and (l). n) A schematic of a nematogel formed by a cellulose network infiltrated by a thermotropic LC without (top) and with an applied electric field *E*. o) Fast switching of the nematogel transparency by electric square-wave pulses that effectively turn *E* on and then off at elapsed times of about 0.1 and 10 ms; the carrier frequency is 50 kHz.

reflection.[49,52] Such orientationally ordered photonic structures are also needed for different parts of the building envelope to control solar gain and emissivity while providing the desired aesthetic appearance at low cost, with only organic materials involved and while manufactured to survive harsh environmental conditions. Bioinspired analogs of such thermal management designs have been recently developed[25,52] and are similar to polarizing optical elements previously fabricated from synthetic LC polymers.[53] Cholesteric LC's helicoidal self-organization (Figure 1e) allows for fabricating nanocellulose-based orientationally ordered photonic materials with designable reflectivity for solar gain control, which can be achieved in infrared without compromising visible-range transparency for window applications.[25] Broadband visible and infrared reflectors with near-100% reflectivity may be designed for thermal management in buildings under different climate conditions. Moreover, to minimize energy loss through thermal conduction, nanocellulose-based materials can be also used to fabricate various types of super-insulating aerogels, including the ones with visible-range transparency.[24,54] Such smart materials can be used to retrofit components of the envelopes in existing buildings, including windows (Figure 1f,g).[24] Importantly, nanocellulose needed for such material applications can be derived from low-cost feedstocks, including wood pulp and waste like the waste of beer production (Figure 1h,i), in the latter case with the help of bacteria (Figure 1j).[25,54–60] When converting waste, one can take advantage of existing technological processes in the food industry.[25,54–58,61,62] Examples involve bacterial biofilms made by *Acetobacter xylinus* or Hansenii[61,62] (Figure 1j) that also make eatable hydrogels for food products like Nata de Coco.

While sources of cellulose are ubiquitous, different types of nanocellulose might be suitable for different building materials. Nanocellulose exhibits hierarchical self-assembly and can come in a variety of different forms.[63] The individual cellulose macromolecules (≈0.4 nm in width) first self-assemble into elementary fibrils with 3–4 nm cross-sections and 1–4 μm length, which then tend to form microfibrils of width >15 nm and fibers with widths in micrometer range and lengths in millimeter range.[63] For the applications discussed here, nanocellulose in the forms of isolated elementary nanofibrils and microfibrils is typically desired.[23–28] The geometry of nanofibers derived from different feedstocks also depends on the source of nanocellulose. For example, elementary nanofibrils derived from wood have lengths of 10–300 nm and diameters of 3–5 nm whereas those produced by bacteria have rectangular 5–10 nm by 30–50 nm cross-sections and 100–1000 nm lengths, though the latter can be modified to achieve sub-10 nm cross-sections.[28] Crystalline regions within cellulose sources are separated by amorphous ones, which allows for breaking them apart into well-defined rod-like nanoparticles. In addition to dimensions, cellulose nanoparticles can have different degrees of crystallinity and both types and orientations of crystallographic lattices, as well as different surface charging and chirality, resulting in physical behavior that depends on the source and preparation of nanocellulose.[28] When produced by bacteria (Figure 1j), the elementary cellulose fibrils tend to stick together via hydrogen bonding to make cellulose fibers. To prevent hydrogen bonding[24,61] between the fibrils, sodium carbomexymethyl cellulose (≈1.5%) can be added to a culture solution. The length-to-width aspect ratio and preparation of anisotropic nanoparticles determine the type (nematic versus cholesteric) of LC colloidal mesophases that form (Figure 1k–m), as well as the concentrations of cellulose nanoparticles at which order-disorder transitions take place (these transitions can occur at <1 wt% for some types of nanocellulose preparations[24,28,46] and at >10 wt% for the other,[42] though most commonly within 1–10 wt%[25,30,40–46]). For the nematic-like order to emerge, the rod-like nanocellulose concentration must be above the critical Onsager concentration[64] for order-disorder transition $c \approx 4/\xi_{\text{eff}}$, where ξ_{eff} is an effective aspect ratio of nanofiber or nanocrystal length to its diameter (larger than the physical diameter due to electrostatic charging and ensuing repulsions).[24,40–46,64] Therefore, the LC self-organization of nanocellulose can be controlled by varying geometric parameters of nanoparticles, pH, surface charging, ionic content, etc.[24,28,30,40–46]). Sections below discuss how nanocellulose with different preparations is used in photonic reflectors and in both transparent and translucent aerogels for applications in different parts of building envelope.

Over 80% of energy generated globally comes from fossil fuels, so making buildings more efficient is key for reducing greenhouse emissions (just the energy lost through windows in the USA is responsible for 70 million tons per year of carbon dioxide emissions) and slowing down climate change.[24,35,36] However, buildings can be also part of safe geoengineering strategies[26] capable of not only mitigating the climate change, but also reducing the local heat waves in densely populated areas. While the areal footprint of buildings increases with growing population, building roofs could be used to reflect unwanted part of solar energy back to space (Figure 1a).[26] Moreover, nanocellulose-based nematogels (gels composed of orientationally ordered nanofibers surrounded by a thermotropic LC of rod-like molecules) can be used to switch between transmission and backscattering of light (Figure 1n,o).[28] In this example, the strong scattering at no fields originates from the large mismatch of the effective refractive index of the thermotropic LC and nanocellulose fibers with high degree of crystallinity within the gel network.[28] While both the nanocellulose and the nematic medium are optically anisotropic, electric rotation of the thermotropic LC's optical axis (director) relative to the average orientation of nanofibers allows for tuning the refractive index mismatch and scattering, with the switching times <1 ms (Figure 1n,o).[28] While nanocellulose can be utilized for many different building technology needs, the discussion below focuses on pre-designed reflectivity and passive thermal barriers.

3. Nanocellulose-Based Photonic Reflectors

Many promising approaches for controlling light involve nanofabricated photonic crystals with periodic spatial variations of dielectric constant.[19] Such structures have also evolved in nature, often to enable thermal management.[1–5] Recently researchers used self-assembly of cellulose nanocrystals to obtain helicoidal organizations that mimic naturally occurring reflectors found in the wings of beetles, like the ones shown in Figure 1d, where reflectivity of these films can be tuned in visible and near-infrared regions (**Figure 2**).[23,25,27,29,42] Colloidal

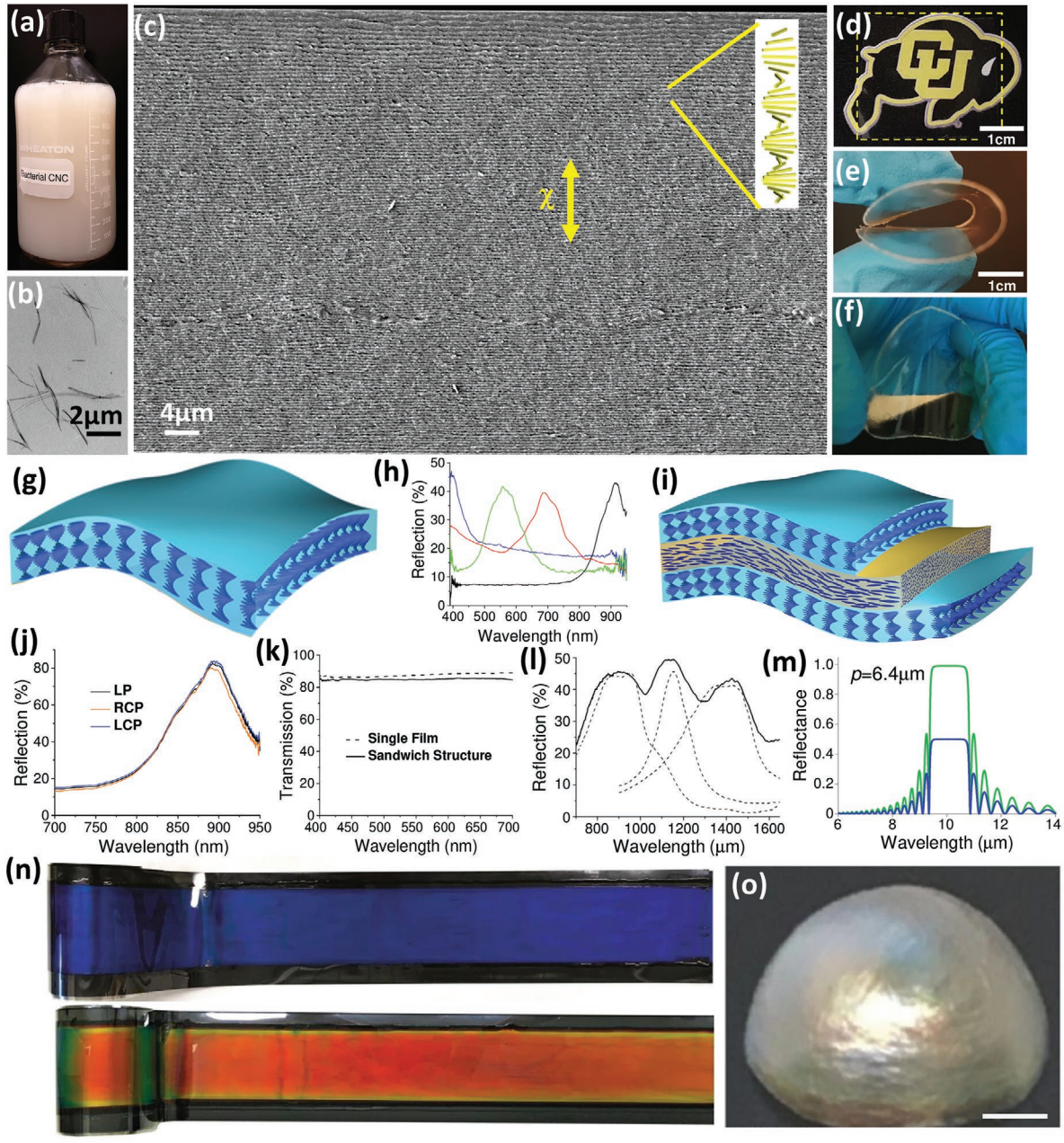

Figure 2. Designable cholesteric photonic reflectors for solar gain and emissivity control. a) A photograph of a concentrated aqueous colloidal dispersion of nanocellulose at ≈10 wt% and b) a TEM image of the nanocellulose particles described in ref. [25]. Note that the colloidal dispersion strongly scatters light due to polydomain helicoidal cholesteric organization and tactoidal domains.[30,39,44,45] c) SEM image of the cholesteric helicoidal structure formed by cellulose nanocrystals obtained in a cross-sectional plane containing the helical axis χ; the distance between periodic stripes is $p/2$ and the inset shows a schematic of the helicoidal configuration of thickness ≈2p. d–f) Demonstration of flexibility and visible transparency of the infrared-reflecting photonic films, which is marked by a dashed square atop of a logo in (d) and flexed in (e,f), with the flexibility enabled by addition of 30 wt% of the plasticizer.[25] g) Schematic of helicoidal cholesteric LC organization. h) Reflection spectra from cholesteric films of different pitch corresponding to Bragg condition satisfied at different visible and near-infrared wavelengths. i) Schematic of three-layer photonic assembly with near-100% reflectivity formed by two cholesteric layers of the same handedness separated by a nematic-like optical retarder, all fabricated from nanocellulose. j) Reflection spectra of a photonic sandwich structure schematically shown in (i) taken for right- and left-handed (RCP, LCP) circular polarization and linear polarization (LP) of incident light. k) Transmission spectrum with natural light incident upon a single film and its corresponding sandwich structure; transmission of a 1 mm thick glass slide is provided for comparison. l) Near-infrared reflection spectra of three individual cholesteric films (dashed lines) and their superposition (solid curve), demonstrating how cellulose-based photonic structures can provide designable photonic reflections for solar gain control. m) Thermal infrared range reflection from a single- and three-layer structures shown in (g,i), respectively, for p = 6.4 μm. n) Rolls of cholesteric films produced with the help of roll-to-roll processing; the width of the rolls is 14 cm. o) Hemispherical cholesteric shell; the scale bar is 1 mm. d,e,g–k) Reproduced with permission.[25] Copyright 2018, American Chemical Society. n) Reproduced under terms of the CC-BY Creative Commons Attribution 4.0 International License (https://creativecommons.org/licenses/by/4.0/).[41] Copyright 2018, The Authors, published by Springer Nature. o) Reproduced with permission.[27] Copyright 2018, Wiley-VCH.

spindle-shaped cellulose nanoparticles (Figure 2a,b) can be prepared from bacterial, wood or other sources. In concentrated aqueous colloidal dispersions, these anisotropic nanoparticles spontaneously self-assemble into a cholesteric LC while continuously rotating around the helical axis χ (Figure 1e), with the distance of 2π-rotation called "helical pitch", p.[30] While p depends on the cellulose source and preparation,[30] drying of solvents within the LC colloids, various types of polymerization and templating allow for transforming these fluid-like cholesterics into solid films with periodic helicoidal structures of nanocrystal orientations (Figure 2c), such as the visibly transparent infrared-reflecting films shown in Figure 2d–f.[25,65–67] Periodicity of these cholesteric structures can be tuned within roughly 0.1–10 μm, for example by locking different pitch values during up to ≈90% pitch shrinkage upon a fabrication process dubbed "evaporation induced self-assembly",[25] which can be further tuned by adding polymers, surfactants, etc. The cross-sectional images in planes containing χ reveal periodic configurations with an effective period of $p/2$ (Figure 2c), consistent with the head-tail symmetry of the nonpolar LC-templated medium. Moreover, nanocellulose colloids can be aligned by magnetic fields and shearing, so that the monodomain LC has a uniform spatial orientation of χ. Cellulose nanoparticles have negative magnetic susceptibility anisotropy and orient orthogonally to the magnetic field,[25] typically directed normal to the film's surface, aligning χ along the surface normal. While such helicoidal structures reflect circularly polarized light matching the handedness of the cholesteric LC (Figure 2g) at the wavelength satisfying the Bragg diffraction condition for given constant p, only up to 50% of unpolarized ambient light can be reflected within a relatively narrow spectral range (Figure 2h).[25] However, the reflection coefficient can be boosted to nearly 100% by designing three-layer sandwich photonic structures that consist of two left-handed cholesteric films separated by an optical retarder (Figure 2i,j), similar to what is found in the exoskeleton of Plusiotis resplendens beetles (such layers in beetles are made of chitin, another abundant biopolymer).[25,52] The overall reflection of the sandwich structure is polarization independent (Figure 2i,j). The left-handed circular polarization component of natural light is selectively reflected by the first cholesteric-like film, through which its right-handed counterpart is transmitted and then converted into left-handed circular polarization mode by the nematic-like half-wave retarder, followed by reflection from the second cholesteric-like layer (Figure 2i).[25] While traversing back, this light reflected from the 2nd cholesteric layer is converted back into right-hand circular polarization mode by the retarder and transmitted through the first left-handed cholesteric-like film (Figure 2i), so that both left- and right-handed components are reflected.[25] The near-100% reflection of the structure is polarization-independent and twofold enhanced as compared to a single cholesteric-like film (Figure 2h,j).[25,52] This reflection is also tunable and can be achieved in the near-infrared range (Figure 2j) while maintaining low <1% haze and high transparency in the visible spectral range (Figure 2k), differently from conventional low-emissivity films (like single and triple silver coatings) that cause tinting.[35,36] Moreover, broadband predesigned reflections can be achieved by introducing spatial gradients of p (see an example in Figure 2c) or superimposing films with different cholesteric configurations, much like in the case of photonic structures in cuticles of beetles (Figure 1d). Figure 2l shows an example of a broadband near-infrared reflection resulting from a sandwich of three like-handed cholesteric films with different p, with the overall spectral reflection being a superposition of reflections due to films of different p (dashed curves). By using achromatic broadband retarders and cholesteric structures with gradients of p, near-100% reflection in entire visible or near infrared range can be achieved by the three-layer (Figure 2i), varying-p structures. Numerical modeling (Figure 2m) of single and three-layer structures for $p = 6.4$ μm shows that these principles can be also applied to design reflections in the spectral range of room-temperature blackbody radiation. However, we note that cellulose is highly absorptive in this spectral range, so double- or triple-templating needs to be utilized to impart such photonic configurations into other materials that are transparent at these wavelengths. Indeed, cellulose nanomaterials serve as a robust templating platform, allowing one to impart the helicoidal assembly onto compatible guest chemicals added to the colloidal dispersion, like a composite containing organosilica and plasticizer added to improve mechanical properties (Figure 2d–f).[25,67] The self-assembly-based fabrication of monodomain cholesteric photonic structures is technological and scalable, with square-meter-range samples already achieved while also taking advantage of roll-to-roll processing (Figure 2n).[41] Much like within cuticles of beetles, such cholesteric films can be fabricated while adopting curvature of various surfaces, like in the case of hemispheres shown in Figure 2o.[23] Dip coating and shearing can also allow for aligning cellulose nanocrystals into nematic-like structures,[25,31] which can serve as a phase retarder, with retardation dependent on the number of successive deposition cycles (also a scalable process).[25] While low emissivity and solar gain control in modern windows are typically achieved in expense of compromising visible-range optical transparency, the near-infrared reflective films based on cholesteric reflectors can feature high transparency across the visible spectrum (Figure 2k).[25] The spectral reflectivity can be designed simply by controlling cholesteric pitch and its gradients within the photonic structures according to the Bragg condition (Figure 2c).[25,52] Combined with the flexibility (Figure 2d–f,n), such photonic materials can be used as films for retrofitting applications and in new insulating glass units and other parts of building envelopes.[25]

Although still at early stages of development, the cholesteric photonic structures may allow for controlling the window's solar heat gain coefficient, the fraction of incident solar energy admitted through a window, including direct transmission and absorption captured by the building. Solar energy can be a free source of heat in the winter but requires extra energy for conditioning during the summer. The designable reflectivity of cholesteric composite films may allow customizing solar heat gain depending on the climate and other factors. Apart from windows, use of such designable reflectors in walls and roofs could also control the solar gain, though here through controlling absorptance and re-radiation into building's interior. Solar reflectance (albedo) and emittance can be optimized to reflect a majority of heat energy, keeping buildings cool. As in the case of photonic structures in beetles with silver- and gold-like reflections (Figure 1d), this potentially can be achieved while defining

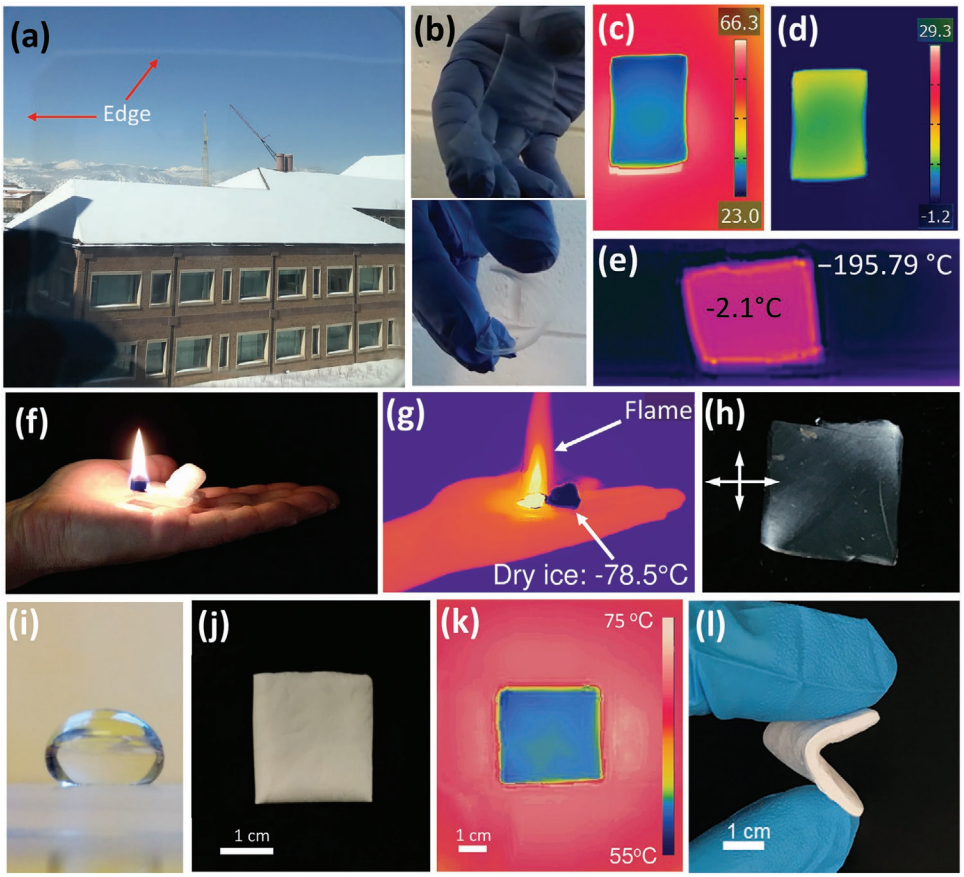

Figure 3. Cellulose-based aerogels. a) A photograph of a transparent aerogel film laminated atop a window pane, with its edges marked by red arrows. b) Frames from a video demonstrating rubber-like flexibility of such aerogels films. These hybrid cellulose-containing aerogel films have density of ≈69 mg cm^{-3} and porosity of ≈95%, fabricated as described in ref. [24]. c–e) Infrared images of the aerogel insulation from a hot plate (c), a cooled surface (d), and a cryogenically cooled surface (e) in room-temperature surroundings. The color-coded temperature (in degrees Celsius) scales in (c,d) and measured surface temperatures in (e) show the thermal barrier capabilities of aerogel films. f,g) Insulation from dry ice and flame held on a hand, as shown in a visible-light (f) and infrared (g) photographs. h) A polarizing photograph of a cellulose–polysiloxane aerogel film placed between crossed polarizers (white double arrow) showing its optical anisotropy due to "frozen" order, similar to that of nematic colloidal dispersion of cellulose nanofibers shown in Figure 1l. i) A photograph of a water droplet atop of a hybrid cellulose-containing aerogel, demonstrating its superhydrophobicity. j–l) Minimally processed translucent cellulose aerogels derived by supercritically drying pellicles of bacterial biofilms grown by *Acetobacter hasenii* shown using visible-light (j,l) and infrared (k) photographs. The photograph in (l) demonstrates the aerogel's flexibility. b,h,i) Reproduced with permission.[24] Copyright 2018, Elsevier.

aesthetically appealing colors of the surfaces of a building envelope, say by mimicking appearance of noble metals (Figure 1d). The bioinspired cellulose-based photonic materials may also enable realization of other highly desired features common to nature, like self-healing.

4. Cellulose-Based Aerogels

Infrared images (Figure 1c) reveal how heat escapes from home and office buildings. Efficient thermal barriers with ultralow thermal conductivity are much needed for all components of building envelopes, including new construction and retrofitting. Aerogels are the porous, low-density solids with ultralow thermal conductivity used in the Mars Rover, pipe insulation, and many other applications, but, so far, rarely in building envelopes (**Figure 3**).[68–72] Thermal conductivity of nonevacuated aerogels can be ≤10 mW K^{-1} m^{-1},[69] much lower than ≈22–32 mW K^{-1} m^{-1} of polyurethane panels (nowadays widely used in building insulation), whereas evacuated aerogels can exhibit thermal conductivity 2–3 mW K^{-1} m^{-1}.[69] While infrared images (Figure 1c) show that windows need insulation the most, conventional aerogels have poor transparency and are often referred to as "frozen smoke" because of the strong light scattering.[68,69] Translucency of aerogels is typically accompanied by haze with bluish color due to "Rayleigh scattering" that is the strongest at shorter wavelengths.[69] Cellulose-based aerogels attracted considerable interest[73–76] and modestly transparent aerogels have been fabricated from colloidal cellulose nanofibers with LC ordering.[76] Recently, transparent hybrid cellulose-based aerogels achieved high >90% transparency and low haze, as needed for window applications (Figure 3a).[24] These hybrid nanocellulose–polysiloxane aerogels are transparent because of their characteristic highly controlled <20 nm sizes of pores and thin nanoparticles with ≈5 nm or smaller diameters (all much smaller than wavelengths of

visible light).[24] Moreover, unlike their fragile silica counterparts, these aerogels are mechanically robust and flexible (Figure 3b). Because of the low thermal conductivity, aerogels effectively insulate from hot and cold surfaces, including the ones at cryogenic temperatures (Figure 3c–e).[24,68,77,78] For example, a transparent aerogel film allows for holding a flame of a starter cube and dry ice at the same time (Figure 3f,g). The ultralow thermal conductivity of aerogels comprises contributions due to gas in pores and the solid network, in addition to the radiation-based one.[67,68,77,78] Pores within the cellulose-based aerogels are considerably smaller than the 60–100 nm "mean free path" of air molecules, so that there is no convection and gas conduction through the air molecules is considerably reduced (a phenomenon known as the "Knudsen Effect") because air molecules collide with the walls of the aerogel's pores more often than with each other.[68,77,78] Since aerogels contain a tiny volume fraction of the solid network (within 0.1–10%) made of nanoparticles with poor thermal contacts, the heat transfer through this network is also small, as is the contribution of the radiative component (negligible at room temperature) because of attenuation of infrared thermal radiation by cellulose's strong absorption and re-emission that gives apparent reflection in this range.[77,78] Since the contribution of solid network to thermal conductivity decreases with increasing porosity whereas that due to air in pores increases, aerogels tend to have a minimum in the thermal conductivity versus porosity dependence.[68,77,78] For cellulose and cellulose-based hybrid aerogels this is within 87–96%, depending on composition, where thermal conductivities ≈10 mW K^{-1} m^{-1} can be achieved,[24,68] comparable to that of other highly insulating organic and silica aerogels.[77,78] Cellulose-based aerogels allow holding dry ice and a burning fire starter cube at the same time on a hand (Figure 3f), demonstrating how such aerogels could be used for insulation in extraterrestrial habitats (building-like conditioned environments outside of the Earth), where surface temperatures of extraterrestrial bodies fluctuate from negative to positive hundreds degrees of Celsius (–125 to 20 °C for Mars and –173 to 127 °C for Moon).[33] Demonstration in Figure 3f,g also shows that the cellulose-containing hybrid aerogels can be fire-retardant, behaving very differently from cellulose itself and aerogels made of cellulose only.

High transparency and low haze of cellulose-based hybrid aerogels originate from their nanoporous structures, with the ordering manifested by birefringence seen when placing the aerogel film between crossed polarizers (Figure 3h).[24] Although cellulose is hydrophilic, nanostructured hybrid aerogels can be made to exhibit super-hydrophobicity (Figure 3i).[24] While transparent aerogels require controlled fabrication procedures, hydrogels of nanocellulose-containing biofilms produced by bacteria like *Acetobacter xylinus* or *Acetobacter hansenii* can be directly converted into broadband-scattering aerogels (Figure 3j-l) with minimal processing by simple solvent exchanges and supercritical drying.[58] Such translucent aerogels could be used in parts of building envelopes different from windows (Figure 1a). A key advantage of cellulose-based aerogels is that their production involves the bottom up approach of colloidal self-assembly. Aqueous colloidal dispersions of cellulose nanofibers can exhibit LC ordering at volume fractions ≤1%, as evidenced by birefringence textures due to spatial variations of the optical axis (director) when observed between cross polarizers (Figure 1k,l).[24,79,80] These ordered structures can be locked in by gelation while preserving the small cross-sections of individual fibers, resulting in monolithic hydrogels, followed by solvent exchange and critical point drying.[24] The nematic order of nanocellulose imparts birefringence to the ensuing aerogels (Figure 3h) with optical anisotropy 5.3×10^{-6}–1.6×10^{-3}, depending on the volume fraction and degree of alignment of the nanofibers.[24] Unidirectional shearing of colloids before gelation provides a robust means of controlling orientation of the optical axis of the effectively optically monocrystalline aerogels, which can be used as retarders in photonic structures like the one shown in Figure 2i.[25]

Cellulose-based hybrid aerogels exhibit mechanical resilience against compressive and bending mechanical deformations (Figure 3b).[24] Such properties allow aerogels to be laminated atop of solid surfaces to retrofit existing single-pane windows (Figure 1f) responsible for the largest fraction of building energy loss.[24] Using transparent aerogels instead of the air gap in double-pane insulating glass units (Figure 1g) could allow for R-10 windows while even reducing their thickness as compared to currently available counterparts. Optical transparency, mechanical flexibility and robustness are among the properties that were historically considered to be incompatible with aerogels, limiting their practical applications, but recent progress in developing cellulose-based aerogels appears to overcome these challenges (Figure 3).[24] In addition, aerogels can be evacuated by removing air from their pores to achieve modest vacuum, which can further boost *R*-values.[81–83] Moreover, the color rendering index for these aerogels is high, over 90%, meaning that colors viewed through such materials remain undistorted.[24] Transparency of aerogels in visible and near infrared ranges could be utilized for passive solar heating, a strategy to maximize the solar gain in a building when heating is desired. Such passive solar systems could harvest solar energy through transparent aerogels and store heat in structures of occupied buildings. Insulated by aerogels, high thermal mass parts of buildings, like concrete slabs, could store large amounts of solar energy absorbed during the day to release it slowly into the building's interior during night. The combination of high visible and near-infrared transparency, spectrally designable reflection and thermal super-insulation was not available previously and now opens many unique opportunities in harnessing, distributing and controlling solar energy delivered to buildings. The recent progress in making aerogels with patterned magnetic domains promises[84] the possibility of magnetic "snap-in" of aerogel films to frames of windows and other parts of building envelopes, though a significant amount of additional research and development is needed to test feasibility and effectiveness of such applications. Aerogels with intermediate and high values of haze can be also useful for daylighting solutions with even illumination of building's interior that also combine thermal insulation with solar gain control,[81–83] which can be made from cellulose (Figure 3j–l).

5. Discussion, Outlook, and Conclusions

Building applications pose stringent requirements in terms of lifetime, durability, aesthetics, fire retardancy, water repellency,

mechanical robustness, scalability and low-cost manufacturing.[35,36] While the sections above discussed how some of these properties have been already achieved in cellulose-based materials, significant additional development is still needed to assure their deployment. Because all discussed cellulose-enabled materials can be made, at least in part, by using dirty feedstocks like waste or abundant resources like wood,[85–88] along with the self-assembly-enabled fabrication and bacteria-based and roll-to-roll processing, technoeconomic analysis shows that their cost can be low (say on the order of a dollar per square foot for transparent aerogel retrofitting films),[24] suitable for applications in buildings. Preliminary durability tests, including UV exposure, humidity, temperature cycling/gradients, reveal no or minimal changes of physical properties, promising that they will meet the stringent requirements for the building envelope materials,[24,25] though many more tests are needed. Although both cholesteric reflectors and aerogels have been fabricated as mechanically robust and flexible films,[24,25] in the latter case already very different from fragile and brittle conventional aerogels,[68,81,82] much more development is needed to assure building-material-grade mechanical performance. For example, the transparent aerogels described in ref. [24] can withstand up to 10–50 kPa compressive stress while exhibiting up to ≈10% elastic deformations (impressive for aerogels),[68,81,82] but would still require protective layers in retrofit products or would have to be placed in-between panes within insulating glass units. Significantly stronger porous materials would be needed in applications where they are directly exposed to building's interior or exterior. Nature again teaches us that it should be possible to fabricate both soft and hard porous and cholesteric-like photonic materials that hybridize organic and inorganic composition and ordered mesoscale structures.[89,90] For example, cholesteric-like porous structures comprising fibrous chitin (the second most abundant biopolymer capable of structural organization similar to that of nanocellulose) in the cuticle of American lobster (*Homarus americanus*) exhibit mechanical property gradients with high stiffness (≈10 GPa) and hardness (130–270 MPa) of exocuticle and smaller stiffness (3–4.5 GPa) and hardness (30–55 MPa) of the endocuticle.[89,90] In addition to re-creating nature's inventions in man-made materials, even more exciting possibility involves direct harnessing natural processes to achieve orderly organizations of hierarchically assembled aligned nanocellulose, an approach that can potentially provide functions ranging from radiative cooling to daylighting with good thermal insulation and potentially even anisotropic thermal conduction.[32,33,85] Aesthetics is a top market driver for most of the building materials, which implies high transparency and color rendering index for windows and a wide range of accessible colors for other parts of the building envelope, which are the properties that can be achieved in the cellulose-based mesostructured materials (Figures 2 and 3).[24,25] Other examples of desired properties include soundproofing, self-healing and self-cleaning of surfaces within roofs and walls. Although these properties are common in nature, achieving them in building envelope presents a major challenge, though they may benefit from invoking nature in fabrication and maintenance as recently even living bricks comprising cyanobacteria have been demonstrated.[91]

The added benefit of using highly insulating retrofit films for windows applications is also the enhancement of condensation resistance of the window. While condensation is not a problem for high-performance windows, temperature of the interior surface of a single-pane window is nearly as low as the outside temperature, causing moisture in the building's interior condense on it. Therefore, boosting window's R-value through aerogel-film-based retrofitting also comes with the side benefit of significantly improved condensation resistance.[24] While energy savings by themselves do not guarantee fast adoption of retrofit products, the side benefits in the forms of condensation resistance and soundproofing boosted by aerogel and reflective film retrofits could be a significant factor in accelerating their market adoption.[92]

The US Department of Energy identified the achievement and market adoption of R-10 windows of thickness/weight comparable to the existing ones as the top-priority goal.[93] Such highly insulating windows have the greatest potential to save energy in both the residential and commercial sectors.[93] While vacuum-insulated glass units are both costly and susceptible to failing of edge seals, transparent aerogels could provide a pathway to achieving this goal provided that low haze ≈1% can be achieved for aerogel slabs of thickness ≈1 in. when integrated with either cholesteric or metal-coating-based low-emissivity films. Another DOE's top-priority target is the insulating building envelope material with ≥R-12 per inch thermal insulation that can be applied to walls to retrofit existing buildings.[93] Both transparent and translucent aerogels (possibly also with cholesteric films to define various colors) could be appropriate for these applications, depending on whether or not passive solar heating is useful for given climate conditions. In addition to passive thermal insulation designs, various dynamic solutions are also of interest[93] and could be enabled by combining ordered nanocellulose structures with thermotropic LCs[28] and colloidal nanoparticle dispersions.[30,94,95]

To conclude, nanocellulose-based materials provide a platform to overcome barriers that hamper building efficiency improvements. Mesostructured cellulose may provide a holistic solution to energy management challenges for buildings to require no or little supplemental heating and cooling for year-round occupant comfort. Depending on the climate- and season-specific needs, they can be pre-designed for capturing or effectively reflecting solar radiation in the visible and near-infrared ranges. These materials could be used both for retrofitting of existing buildings and in new construction. Inexpensive abundant source materials (including waste converted into cellulose by bacteria) and the use of colloidal self-assembly in fabrication of designable reflectors and aerogels are key aspects of low-cost and fabrication scalability.[24,25] Beyond buildings, transparent aerogel and designable reflectors discussed here are also needed for greenhouse applications, protective cloth, etc. The use of energy-efficient cellulose-based materials in the buildings and related sectors may allow for reducing energy consumption and greenhouse gas emissions. Moreover, by nanoscale templating, judicious control of nanoscale structure and chemical composition, cellulose-enabled mesostructured materials for many other applications can be achieved.

Acknowledgements

I.I.S. thanks his students and postdocs working on the research projects related to this research news review, including E. Abraham, V. Chandrasekar, V. Cherpak, J. De La Cruz, B. Fleury, A.W. Frazier, A.J. Funk, A. Hess, Y. Jiang, T. Lee, Y. Li, Q. Liu, D. Liu, S. G. Morrison, K. Reddy Peddireddy, B. Senyuk, J. B. Ten Hove and H. Zhou. I.I.S. acknowledges discussions with B. Borak, T. Culp, P. Finch, J. Gerbi, E. Schiff, M. Sofos and M. Yamada. I.I.S. thanks to Catalyst Paper for donating never dried wood pulp used in some of the research discussed within this review. This research was partially supported by the U.S. Department of Energy, Advanced Research Projects Agency-Energy award DE-AR0000743.

Conflict of Interest

The author declares no conflict of interest.

Keywords

aerogels, broadband reflectors, buildings, liquid crystal, nanocellulose, photonic structure

Received: February 21, 2020
Revised: March 21, 2020
Published online:

[1] P. Vukusic, J. R. Sambles, *Nature* **2003**, *424*, 852.
[2] I. Medina, E. Newton, M. R. Kearney, R. A. Mulder, W. P. Porter, D. Stuart-Fox, *Nat. Commun.* **2018**, *9*, 3610.
[3] E. D. Finlayson, L. T. McDonald, P. Vukusic, *J. R. Soc., Interface* **2017**, *14*, 20170129.
[4] D. Stuart-Fox, E. Newton, S. Clusella-Trullas, *Phil. Trans. R. Soc. B* **2017**, *372*, 20160345.
[5] E. B. Knipling, *Remote Sens. Environ.* **1970**, *1*, 155.
[6] X. Jin, J. Zhang, C. Hurren, J. Li, R. Rajkhowa, X. Wang, *Text. Res. J.* **2016**, *86*, 1935.
[7] A. R. Parker, *J. Opt. A: Pure Appl. Opt.* **2000**, *2*, R15.
[8] M. E. McNamara, D. E. G. Briggs, P. J. Orr, H. Noh, H. Cao, *Proc. R. Soc. B* **2012**, *279*, 1114.
[9] A. Dance, *Proc. Natl. Acad. Sci. USA* **2016**, *113*, 8552.
[10] M. E. McNamara, D. E. G. Briggs, P. J. Orr, S. Wedmann, H. Noh, H. Cao, *PLoS Biol.* **2011**, *9*, 1001200.
[11] M. E. McNamara, D. E. G. Briggs, P. J. Orr, N. S. Gupta, E. R. Locatelli, L. Qiu, H. Yang, Z. Wang, H. Noh, H. Cao, *Geology* **2013**, *41*, 487.
[12] A. R. Parker, D. R. McKenzie, *Proc. Biol. Sci.* **2003**, *270*, S151.
[13] M. E. McNamara, D. E. G. Briggs, P. J. Orr, D. J. Field, Z. Wang, *Biol. Lett.* **2013**, *9*, 20130184.
[14] J. Vinther, D. E. G. Briggs, J. Clarke, G. Mayr, R. O. Prum, *Biol. Lett.* **2010**, *6*, 128.
[15] Q. Li, K.-Q. Gao, Q. Meng, J. A. Clarke, M. D. Shawkey, L. D'Alba, R. Pei, M. Ellison, M. A. Norell, J. Vinther, *Science* **2012**, *335*, 1215.
[16] R. Hooke, *Micrographia*, Martyn and Allestry, London, UK **1665**.
[17] I. Newton, *Opticks*, 4th ed., Dover, New York **1730**.
[18] A. A. Michelson, *Philos. Mag.* **1911**, *21*, 554.
[19] J. Joannopoulos, S. G. Johnson, *Photonic Crystals: The Road from Theory to Practice*, Springer, New York **2002**.
[20] N. N. Shi, C.-C. Tsai, F. Camino, G. D. Bernard, N. Yu, R. Wehner, *Science* **2015**, *349*, 298.
[21] A. P. Raman, M. A. Anoma, L. Zhu, E. Rephaeli, S. Fan, *Nature* **2014**, *515*, 540.
[22] W. Li, S. Fan, *Opt. Express* **2018**, *26*, 15995.
[23] M. Chekini, E. Prince, L. Zhao, H. Mundoor, I. I. Smalyukh, E. Kumacheva, *Adv. Opt. Mater.* **2020**, *8*, 1901911.
[24] Q. Liu, A. W. Frazier, X. Zhang, J. De La Cruz, R. Yang, A. Hess, I. I. Smalyukh, *Nano Energy* **2018**, *48*, 266.
[25] J. De La Cruz, Q. Liu, A. W. Frazier, B. Senyuk, I. I. Smalyukh, *ACS Photonics* **2018**, *5*, 2468.
[26] H. Akbari, H. D. Matthews, D. Seto, *Environ. Res. Lett.* **2012**, *7*, 024004.
[27] P. Rofouie, M. Alizadehgiashi, H. Mundoor, I. I Smalyukh, E. Kumacheva, *Adv. Funct. Mater.* **2018**, *28*, 1803852.
[28] Q. Liu, I. I. Smalyukh, *Sci. Adv.* **2017**, *3*, 1700981.
[29] M. Gu, C. Jiang, D. Liu, X. Cao, W. Gustave, I. I. Smalyukh, *ACS Appl. Mater. Interfaces* **2016**, *8*, 32565.
[30] Q. Liu, M. Campbell, J. S. Evans, I. I. Smalyukh, *Adv. Mater.* **2014**, *26*, 7178.
[31] M. Campbell, Q. Liu, A. Sanders, J. S. Evans, I. I. Smalyukh, *Materials* **2014**, *7*, 3021.
[32] T. Li, M. Zhu, Z. Yang, J. Song, J. Dai, Y. Yao, W. Luo, G. Pastel, B. Yang, L. Hu, *Adv. Energy Mater.* **2016**, *6*, 1601122.
[33] T. Li, Y. Zhai, S. He, W. Gan, Z. Wei, M. Heidarinejad, D. Dalgo, R. Mi, X. Zhao, J. Song, J. Dai, C. Chen, A. Aili, A. Vellore, A. Martini, R. Yang, J. Srebric, X. Yin, L. Hu, *Science* **2019**, *364*, 760.
[34] R. Wordsworth, L. Kerber, C. Cockell, *Nat. Astron.* **2019**, *3*, 898.
[35] L. Pérez-Lombard, J. Ortiz, C. Pout, *Energy Build.* **2008**, *40*, 394.
[36] W. Chung, *Appl. Energy* **2011**, *88*, 1470.
[37] B. Frka-Petesic, S. Vignolini, *Nat. Photonics* **2019**, *13*, 365.
[38] S. Vignolini, P. J. Rudall, A. V. Rowland, A. Reed, E. Moyroud, R. B. Faden, J. J. Baumberg, B. J. Glover, U. Steiner, *Proc. Natl. Acad. Sci. USA* **2012**, *109*, 15712.
[39] J. P. F. Lagerwall, C. Schutz, M. Salajkova, J. H. Noh, J. H. Park, G. Scalia, L. Bergstrom, *NPG Asia Mater.* **2014**, *6*, 80.
[40] A. Isogai, T. Saito, H. Fukuzumi, *Nanoscale* **2011**, *3*, 71.
[41] H.-L. Liang, M. M. Bay, R. Vadrucci, C. H. Barty-King, J. Peng, J. J. Baumberg, M. F. L. De Volder, S. Vignolini, *Nat. Commun.* **2018**, *9*, 4632.
[42] C. Li, J. Evans, N. Wang, T. Guo, S. He, *Sci. Rep.* **2019**, *9*, 11290.
[43] K. E. Shopsowitz, H. Qi, W. Y. Hamad, M. J. MacLachlan, *Nature* **2010**, *468*, 422.
[44] C. Honorato-Rios, A. Kuhnhold, J. R. Bruckner, R. Dannert, T. Schilling, J. P. F. Lagerwall, *Front. Mater.* **2016**, *3*, 21.
[45] R. M. Parker, G. Guidetti, C. A. Williams, T. Zhao, A. Narkevicius, S. Vignolini, B. Frka-Petesic, *Adv. Mater.* **2018**, *30*, 1704477.
[46] M. Zhao, F. Ansari, M. Takeuchi, M. Shimizu, T. Saito, L. A. Berglund, A. Isogai, *Nanoscale Horiz.* **2018**, *3*, 28.
[47] W. E. Vargas, E. Avendano, M. Hernández-Jiménez, D. E. Azofeifa, E. Libby, Á. Solís, C. Barboza-Aguilar, *Biomimetics* **2018**, *3*, 30.
[48] C. Campos-Fernández, D. E. Azofeifa, M. Hernández-Jiménez, A. Ruiz-Ruiz, W. E. Vargas, *Opt. Mater. Express* **2011**, *1*, 85.
[49] J. Hwang, M. H. Song, B. Park, S. Nishimura, T. Toyooka, J. W. Wu, Y. Takanishi, K. Ishikawa, H. Takezoe, *Nat. Mater.* **2005**, *4*, 383.
[50] M.H. Song, B. Park, K.-C. Shin, T. Ohta, Y. Tsunoda, H. Hoshi, Y. Takanishi, K. Ishikawa, J. Watanabe, S. Nishimura, T. Toyooka, Z. Zhu, T.M. Swager, H. Takezoe, *Adv. Mater.* **2004**, *16*, 779.
[51] R. J. Moon, A. Martini, J. Nairn, J. Simonsenf, J. Youngblood, *Chem. Soc. Rev.* **2011**, *40*, 3941.
[52] S. N. Fernandes, P. L. Almeida, N. Monge, L. E. Aguirre, D. Reis, C. L. P. de Oliveira, A. M. F. Neto, P. Pieranski, M. H. Godinho, *Adv. Mater.* **2017**, *29*, 1603560.
[53] D. J. Broer, J. Lub, G. N. Mol, *Nature* **1995**, *378*, 467.
[54] W. Y. Hamad, T. Q. Hu, *Can. J. Chem. Eng.* **2010**, *88*, 392.
[55] Y. Habibi, L. A. Lucia, O. J. Rojas, *Chem. Rev.* **2010**, *110*, 3479.
[56] M. Giese, L. K. Blusch, M. K. Khan, M. J. MacLachlan, *Angew. Chem., Int. Ed.* **2015**, *54*, 2888.
[57] J. Pan, W. Y. Hamad, S. K. Straus, *Macromolecules* **2010**, *43*, 3851.

[58] E. Abraham, B. Fleury, V. Chandrasekar, Q. Liu, J. De La Cruz, B. Senyuk, I. I. Smalyukh, unpublished.
[59] A. J. Hess, I. I. Smalyukh, Q. Liu, J. A. De La Cruz, B. Fleury, E. Abraham, V. Cherpak, B. Senyuk, *US 16/017319*, **2019**.
[60] A. J. Hess, Q. Liu, I. I. Smalyukh, *US 15/868714*, **2018**.
[61] R. M. Brown, J. H. Willison, C. L. Richardson, *Proc. Natl. Acad. Sci. USA* **1976**, *73*, 4565.
[62] W. S. Williams, R. E. Cannon, *Appl. Environ. Microbiol.* **1989**, *55*, 2448.
[63] W. Czaja, D. Romanovicz, R. M. Brown, *Cellulose* **2004**, *11*, 403.
[64] L. Onsager, *Ann. N. Y. Acad. Sci.* **1949**, *51*, 627.
[65] K. E. Shopsowitz, W. Y. Hamad, M. J. MacLachlan, *J. Am. Chem. Soc.* **2012**, *134*, 867.
[66] J. Majoinen, E. Kontturi, D. G. Gray, *Cellulose* **2012**, *19*, 1599.
[67] T. Asefa, M. J. MacLachlan, N. Coombs, G. A. Ozin, *Nature* **1999**, *402*, 867.
[68] a) A. C. Pierre, G. M. Pajonk, *Chem. Rev.* **2002**, *102*, 4243; b) M. Aegerter, N. Leventis, M. M. Koebel, *Aerogels Handbook*, Springer Science & Business Media, New York **2011**.
[69] R. Baetens, B. P. Jelle, A. Gustavsen, *Energy Build.* **2011**, *43*, 761.
[70] K. Kanamori, K. Nakanishi, *Chem. Soc. Rev.* **2011**, *40*, 754.
[71] T. Shimizu, K. Kanamori, A. Maeno, H. Kaji, K. Nakanishi, *Langmuir* **2016**, *32*, 13427.
[72] G. Hasegawa, T. Shimizu, K. Kanamori, A. Maeno, H. Kaji, K. Nakanishi, *Chem. Mater.* **2017**, *29*, 2122.
[73] F. Fischer, A. Rigacci, R. Pirard, S. Berthon-Fabry, P. Achard, *Polymer* **2006**, *47*, 7636.
[74] J. Cai, S. Liu, J. Feng, S. Kimura, M. Wada, S. Kuga, L. Zhang, *Angew. Chem.* **2012**, *124*, 2118.
[75] G. Hayase, K. Kanamori, K. Abe, H. Yano, A. Maeno, H. Kaji, K. Nakanishi, *ACS Appl. Mater. Interfaces* **2014**, *6*, 9466.
[76] Y. Kobayashi, T. Saito, A. Isogai, *Angew. Chem., Int. Ed.* **2014**, *53*, 10394.
[77] X. Lu, M. C. Arduini-Schuster, *Science* **1992**, *255*, 971.
[78] Z. Y. Li, H. Liu, X. P. Zhao, W. Q. Tao, *J. Non-Cryst. Solids* **2015**, *430*, 43.
[79] G. J. Vroege, H. N. W. Lekkerkerker, *Rep. Prog. Phys.* **1992**, *55*, 1241.
[80] H. Fukuzumi, R. Tanaka, T. Saito, A. Isogai, *Cellulose* **2014**, *21*, 1553.
[81] J. M. Schultz, K. I. Jensen, *Vacuum* **2008**, *82*, 723.
[82] U. Berardi, *Appl. Energy* **2015**, *154*, 603.
[83] P. Thapliyal, K. Singh, *J. Mater. Sci.* **2014**, *2014*, 127049.
[84] Y. Li, Q. Liu, A. J. Hess, S. Mi, X. Liu, Z. Chen, Y. Xie, I. I. Smalyukh, *ACS Nano* **2019**, *13*, 13875.
[85] M. Zhu, Y. Wang, S. Zhu, L. Xu, C. Jia, J. Dai, J. Song, Y. Yao, Y. Wang, Y. Li, D. Henderson, W. Luo, H. Li, M. L. Minus, T. Li, L. Hu, *Adv. Mater.* **2017**, *29*, 1606284.
[86] E. Tsouko, C. Kourmentza, D. Ladakis, N. Kopsahelis, I. Mandala, S. Papanikolaou, F. Paloukis, V. Alves, A. Koutinas, *Int. J. Mol. Sci.* **2015**, *16*, 14832.
[87] Z. Li, L. Wang, J. Hua, S. Jia, J. Zhang, H. Liu, *Carbohydr. Polym.* **2015**, *120*, 115.
[88] S. Keshk, *J. Bioprocess. Biotech.* **2014**, *04*, 2.
[89] M. Mitov, *Soft Matter* **2017**, *13*, 4176.
[90] D. Raabe, C. Sachs, P. Romano, *Acta Mater.* **2005**, *53*, 4281.
[91] C. M. Heveran, S. L. Williams, J. Qiu, J. Artier, M. H. Hubler, S. M. Cook, J. C. Cameron, W. V. Srubar III, *Matter* **2020**, *2*, 481.
[92] *Single-Pane Highly Insulating Efficient Lucid Designs (SHIELD)*, U. S. Department of Energy, **2015**, *Funding Opportunity No. DE-FOA-0001425*, CFDA Number 81.135. K.
[93] K. Sawyer, *R&D Roadmap for Emerging Window and Building Envelope Technologies*, U. S. Department of Energy, **2014**.
[94] G. H. Sheetah, Q. Liu, B. Senyuk, B. Fleury, I. I. Smalyukh, *Opt. Express* **2018**, *26*, 22264.
[95] Q. Liu, Y. Yuan, I. I. Smalyukh, *Nano Lett.* **2014**, *14*, 4071.